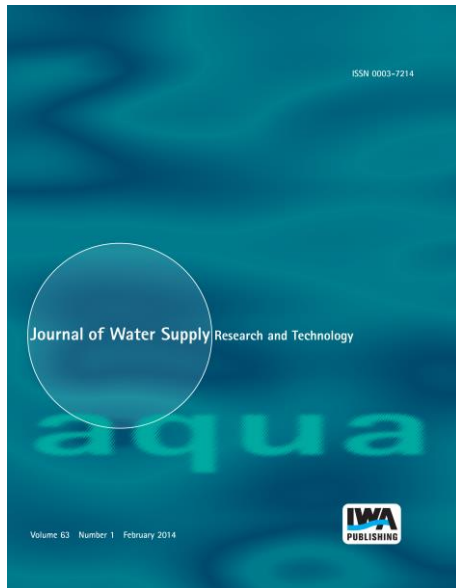


ELECTRONIC OFFPRINT

Use of this pdf is subject to the terms described below



This paper was originally published by IWA Publishing. The author's right to reuse and post their work published by IWA Publishing is defined by IWA Publishing's copyright policy.

If the copyright has been transferred to IWA Publishing, the publisher recognizes the retention of the right by the author(s) to photocopy or make single electronic copies of the paper for their own personal use, including for their own classroom use, or the personal use of colleagues, provided the copies are not offered for sale and are not distributed in a systematic way outside of their employing institution. **Please note that you are not permitted to post the IWA Publishing PDF version of your paper on your own website or your institution's website or repository.**

If the paper has been published "Open Access", the terms of its use and distribution are defined by the Creative Commons licence selected by the author.

Full details can be found here: <http://iwaponline.com/content/rights-permissions>

Please direct any queries regarding use or permissions to aqua@iwap.co.uk

Resilience-based water main rehabilitation planning in a multi-hazard context

Zeinab Farahmandfar and Kalyan R. Piratla

ABSTRACT

Due to aging beyond the intended design life, many water mains in the USA are currently deteriorated resulting in an increasing number of failures which challenge water utilities with diminished supply reliabilities, loss of treated water, and numerous other societal issues. Water pipeline systems serving regions that are naturally vulnerable to external hazards, such as earthquakes, pose additional challenges. Numerous vulnerabilities such as these must be congruently analyzed for optimal capital improvement planning of water supply systems. A resilience-based rehabilitation planning framework is presented and demonstrated in this paper to coherently integrate the vulnerabilities of water pipelines to seismic hazards and natural deterioration. The artificial bee colony (ABC), shuffled frog leaping (SFLA), and genetic algorithms (GA) are investigated to identify the best performing optimization algorithm to be used in the modeling framework presented in this study. A scenario of a real-world water supply system operating in the earthquake-prone region in South Carolina is used for demonstrating the rehabilitation framework. The study approach and the presented findings will provide guidance to water utility professionals in optimal capital improvement planning to enhance supply resilience to a multitude of vulnerabilities.

Key words | decision-making tools, seismic resilience, water pipeline rehabilitation

Zeinab Farahmandfar
Kalyan R. Piratla (corresponding author)
Glenn Department of Civil Engineering,
Clemson University,
Clemson, SC 29634,
USA
E-mail: *kpiratl@clemson.edu*

INTRODUCTION

Inadequate funding devoted to water infrastructure maintenance over the past several decades has led to the current state of pipeline deterioration that is increasingly threatening the supply reliability goals of water utilities in the USA. A clear indicator of the critical state of water infrastructure is the increasing number of water main failures reported from all across the nation (ASCE 2017). Furthermore, water utilities operating in regions that are uniquely vulnerable to certain external hazards, such as earthquakes or landslides, need to be cognizant of the potential impacts and carefully consider them in capital improvement planning. Increasing water demands is another universal challenge influencing capital improvement planning by water utilities. A multitude of vulnerabilities such as these

ought to be coherently integrated for planning purposes. The majority of the future capital improvement works in water supply systems (WSSs) will expectedly involve pipeline rehabilitation projects, and consequently, it is important to formulate a rehabilitation decision-making framework that will coherently integrate multiple vulnerabilities to result in more resilient WSSs. Such a framework is presented and demonstrated in this paper. An aging coastal WSS serving a seismically active region with an increasing consumer base is chosen for demonstrating the rehabilitation planning framework. The proposed rehabilitation planning framework is informed by an evolutionary optimization algorithm that maximizes water supply resilience to both pipeline deterioration and multiple seismic hazards.

PREVIOUS RESEARCH

Considerable efforts were devoted to developing rehabilitation frameworks for WSSs in the past. The majority of the past studies used statistical modeling to forecast pipeline deterioration trends into the future and subsequently identified the critical rehabilitation needs within budgetary constraints. The statistical deterioration models assumed various forms. For example, [Shamir & Howard \(1979\)](#) used an exponential model that determined the pipeline break rate based on its age to estimate the optimal timing of pipeline replacement at least cost. [Walski & Pelliccia \(1982\)](#) later accounted for the influence of pipeline diameter and known previous breaks and developed a similar exponential relationship as [Shamir & Howard \(1979\)](#). [Andreou *et al.* \(1987\)](#) presented two regression models to relate pipeline fragility (or failure probability) with its age. They used a proportional hazards model for the early life cycle stage and a Poisson-type model for the later stage.

Another group of studies used the hydraulic capabilities of the system in addition to the statistical derivations to determine rehabilitation timing of pipelines. Many such studies integrated optimization programs with hydraulic simulation tools. For example, [Woodburn *et al.* \(1987\)](#) connected a nonlinear optimization program with KYPIPE to identify the pipeline renewal needs at least cost. [Halhal *et al.* \(1997\)](#) similarly connected a multi-objective messy genetic algorithm (GA) with EPANET program to congruently minimize costs and maximize hydraulic benefits while determining the pipeline renewal needs. [Dandy & Engelhardt \(2001\)](#) scheduled pipeline replacement and also determined the new diameters using an integrated optimization-simulation framework. [Dandy & Engelhardt \(2006\)](#) later used a multi-objective GA to develop cost vs. reliability trade-off curves for choosing pipeline rehabilitation options. [Nafi & Kleiner \(2010\)](#) also employed a multi-objective GA for identifying and planning pipeline replacement needs synergistically with known road works. [Yoo *et al.* \(2014\)](#) recently presented a framework for prioritizing pipeline rehabilitation needs based on both deterioration rate and hydraulic considerations. They accounted for internal and external pipeline stressors in their framework.

Although several previous studies presented rehabilitation planning frameworks for WSSs, not many considered

multiple hazards and the resulting vulnerabilities. An exception is the study of [Yoo *et al.* \(2014\)](#), which considered seismic and deterioration hazards in an integrated manner. They, however, used a simplified multi-criteria decision-making method for deterioration modeling and also did not employ an optimization model for determining the effective rehabilitation strategies. Their assumption of a limited number of pipeline failures in seismic events is also unjustified. This paper attempts to address some of these gaps in the body of knowledge on water pipeline rehabilitation planning.

STUDY METHODOLOGY

Water pipeline rehabilitation programs are complex capital improvement works involving considerable expense and it is therefore imperative to maximize the resulting benefits with least cost. Evolutionary optimization algorithms are proposed to serve water main rehabilitation planning. Traditionally, water supply reliability has been a crucial goal in the design or rehabilitation of water distribution networks. It is, however, computationally challenging to quantify supply reliability and integrate it with optimization programs, especially for large WSSs. Consequently, numerous surrogate measures of supply reliability referred to as resilience metrics have been proposed and demonstrated ([Todini 2000](#); [Tanyimboh & Templeman 2000](#); [Prasad & Park 2004](#); [Cimellaro *et al.* 2015](#)). Using a previously demonstrated resilience metric, a rehabilitation planning framework is presented in this paper to maximize WSS resilience to two different uncertainties, namely, pipeline deterioration and seismic vulnerability. Predicted growth in water demand has also been accounted for in the proposed rehabilitation framework.

Resilience analysis

A previously proposed flow-based resilience metric, presented in Equation (1), is used for quantifying WSS resilience in this study ([Farahmandfar *et al.* 2015](#)). The resilience metric appropriately blends both robustness and redundancy dimensions of the 4R-Resilience approach presented by [Bruneau *et al.* \(2003\)](#). Pipeline availability

$(1 - P_{fj})$ represents robustness while nodal degree ($\sum_{j=1}^{N_i} (1 - P_{fj})$) and buffer nodal head ($h_{i,t} - h_{i,t}^*$) characterize the redundancy available in the WSS (Farahmandfar *et al.* 2015):

$$R = \frac{\sum_{t=1}^{td} \sum_{i=1}^{N_n} \left(\left(\sum_{j=1}^{N_i} (1 - P_{fj}) \right) q_{i,t}^* (h_{i,t} - h_{i,t}^*) \right)}{4 \times \sum_{t=1}^{td} \sum_{i=1}^{N_n} q_{i,t}^* h_{i,t}^*} \quad (1)$$

where R is the resilience value; td is the number of time steps in the demand pattern of the studied WSS; N_n is the total number of nodes; N_i is the total number of links connected to node i ; P_{fj} is the failure probability of link j ; $q_{i,t}^*$ is the demand of node i in time step t in liters per min (1 liter = 0.26 gallons); $h_{i,t}$ is the actual total head at node i in time step t in m (1 m = 3.28 ft); and $h_{i,t}^*$ is the minimum required total head at node i in time step t in m.

Rehabilitation framework

The proposed rehabilitation framework employs an evolutionary optimization algorithm to determine the optimal set of pipeline rehabilitation actions that will maximize WSS resilience subjected to budget and other physical constraints (Farahmandfar 2016). In order to be able to use the flow-based resilience metric from Equation (1), pipeline fragility analysis is carried out for both single and multiple hazard scenarios to derive individual and integrated pipeline failure probabilities. Pipeline deterioration and earthquakes are considered as the two hazards in this study.

WSS resilience, calculated using Equation (1), can be improved through either strengthening the pipelines (i.e., increasing robustness) or adding more hydraulic energy (i.e., redundancy). Therefore, any pipeline could be left as it is or rehabilitated using one of the following methods: (a) relining, (b) replacement with the same diameter pipeline, or (c) replacement with a larger diameter pipeline. Relining provides smoother internal surface with an increased Hazen–Williams coefficient (C) while, at the same time, protects the pipeline from further corrosion if it is a metallic or reinforced concrete pipe. Several lining technologies, such as epoxy lining and polyurethane lining, are becoming increasingly popular and complementary to the conventional cement mortar lining for water pipeline rehabilitation (Deb

et al. 2010). Additionally, cured-in-place-pipe (CIPP) and close-fit slip lining are other popular lining alternatives that offer structural enhancement in addition to the hydraulic benefits (Piratla *et al.* 2016). It is assumed in this study that cement mortar lining would be used for non-structural pipe rehabilitation due to its wide popularity in North America (Deb *et al.* 2010); as a result, only the improvement in C value is accounted for in this study while using cement mortar lining. Pipeline replacement (i.e., both with the same diameter or larger diameter pipeline) entails installing a new pipeline in place of the deteriorated pipeline using either an open-cut or a trenchless construction method. Pipe bursting is a trenchless replacement method that not only requires minimal excavation (Selvakumar *et al.* 2002), but is also shown to be environmentally friendly (Ariaratnam & Sihabuddin 2009; Ariaratnam *et al.* 2013). Pipeline replacement is expected to enhance its structural integrity and also improve the hydraulic capacity (Kleiner *et al.* 1998). It is less practical to drastically upsize an existing pipeline and therefore it is assumed in this study that ‘replacement with larger diameter’ option installs a new pipeline with a diameter upsize of 101.6 mm (or 4 inches). In order to evaluate the influence of each candidate solution resulting from the optimization algorithm on WSS resilience, a hydraulic simulation model of WSSs developed using EPANET 2.0 (Rossman 2000) software is coupled with the optimization algorithm. The overall rehabilitation cost (C_O) is calculated using the following equation:

$$C_O = \sum_{i=1}^{N_r} C_i(D_i, L_i) + \sum_{j=1}^{N_l} C_j(D_j, L_j) \quad (2)$$

where N_r is the number of links chosen to be replaced; $C_i(D_i, L_i)$ is the cost of replacing pipe i of length L_i with diameter D_i ; N_l is the number of pipelines chosen to be relined; $C_j(D_j, L_j)$ is the cost of relining pipe j of length L_j and diameter D_j .

Several evolutionary optimization algorithms, such as GA, have been used in the past for water main rehabilitation planning (Halhal *et al.* 1997; Dandy & Engelhardt 2001; Nafi & Kleiner 2010). Other comparable algorithms popularly used for non-linear optimization problems include shuffled frog leaping algorithm (SFLA) and artificial bee colony (ABC), which were reported to have performed better than or on a par with GA (Karaboga & Akay 2009). This study

tested these three algorithms to determine the best-suited one for use in the proposed rehabilitation framework.

Pipeline fragility analysis

Water pipeline deterioration has been popularly classified into structural and functional deterioration (Kleiner & Rajani 2001). Structural deterioration weakens the pipeline either through loss of thickness or other defects that diminishes the ability to withstand stresses. On the other hand, functional deterioration diminishes the hydraulic capacity through higher frictional losses. Structural pipeline deterioration, which has been the primary focus in the relevant literature, leads to increasing failures of a pipeline. The estimated repair rate (RR^D) of a pipeline from structural deterioration is calculated in this study using previously developed regression models presented in Wang *et al.* (2009). Wang *et al.* (2009) developed deterioration models that related estimated annual repair rates of pipelines to their material, diameter, length, and age. Their models are presented in Equations (3)–(5) for cast iron (CI), lined ductile iron (DI), and PVC pipelines, respectively. Due to the usage of logarithm functions, Equations (3)–(5) cannot be used to estimate repair rates of replaced pipelines with an age value of zero. The deterioration model presented in Equation (6) has been used to estimate pipeline repair rates post-replacement (Alvisi & Franchini 2006).

$$\begin{aligned} \log RR_i^D = & 4.85 - 0.021 \log age_i + 0.000245 \log age_i^2 \\ & + 0.00281 D_i - 0.905 \log L_i - 1.4 \log D_i \end{aligned} \quad (3)$$

$$\begin{aligned} \log RR_i^D = & 3.36 + 0.00015 L_i \times \log age_i - 1.11 \log L_i \\ & - 0.646 \log age_i - 0.254 \log D_i \end{aligned} \quad (4)$$

$$\log RR_i^D = 2.69 - 0.898 \log L_i - 0.745 \log age_i \quad (5)$$

where RR_i^D is the repair rate of pipe i due to deterioration ($\text{km}^{-1} \text{year}^{-1}$); age_i is the age of pipe i (year); L_i is the length of pipe i in m; and D_i is the diameter of pipe i in mm.

$$RR_i^{D,0} = \beta e^{-xD_i} \quad (6)$$

where $RR_i^{D,0}$ is the repair rate of the replaced pipe i (with age equal to zero) due to deterioration ($\text{km}^{-1} \text{year}^{-1}$); and

β and x are coefficients that are, respectively, considered to be 0.269 and 0.0023, as suggested by Alvisi & Franchini (2006). These parametric values ensure that the fragility post-rehabilitation is less than that prior to it (Farahmandfar 2016).

On the other hand, estimated pipeline repair rates (RR^S) due to modeled seismic hazards are calculated using probability of significant liquefaction as follows (ALA 2009; Farahmandfar *et al.* 2016):

$$RR^S = (1 - P_{Liq})RR_{TGD} + P_{Liq} RR_{PGD} \quad (7)$$

where P_{Liq} (or P_{LPI}) is the probability of liquefaction in percent obtained from a liquefaction potential map; RR_{TGD} and RR_{PGD} are the number of estimated repairs ($\text{km}^{-1} \text{year}^{-1}$) due to transient ground deformations (TGD) and permanent ground deformations (PGD) hazards, respectively.

A detailed description of these two primary types of seismic hazards for buried pipelines and the procedures used to estimate RR_{TGD} and RR_{PGD} are presented in Farahmandfar *et al.* (2016). The following equations are used to estimate RR_{TGD} and RR_{PGD} (Farahmandfar *et al.* 2016):

$$RR_{TGD} = K_1 K_t \times 0.00241 \times PGV \quad (8)$$

$$RR_{PGD} = K_2 K_t \times 2.58 \times PGD^{0.319} \quad (9)$$

where PGV is peak ground velocity in cm/sec (1 cm = 0.39 inch); PGD is permanent ground deformation in cm; K_1 , K_2 , and K_t are correction factors for pipe size, material, and current structural health, as discussed in Farahmandfar *et al.* (2016). K_1 is 1, 0.5, and 0.5 while K_2 is 1, 0.8, and 0.5 for CI, polyvinyl chloride (PVC), and DI pipe materials, respectively (Farahmandfar *et al.* 2016).

The pipeline fragility (or failure probability) due to individual hazards is estimated using Equations (10) and (11) assuming that the repair rates follow Poisson probability distribution (Su *et al.* 1987; Fragiadakis & Christodoulou 2014).

Pipeline fragility indicates the probability of having at least one failure on a given pipe segment:

$$P_{fj}^D = 1 - e^{-RR_i^D * L_i} \quad (10)$$

$$P_{fj}^S = 1 - e^{-RR_j^S * L_j} \quad (11)$$

where P_{fj}^D is the failure probability of pipeline j due to deterioration; and P_{fj}^S is the failure probability of pipeline j due to seismic hazard.

Integrated pipeline fragilities for combined loading of deterioration and seismic hazards are estimated using the following equation based on the Wen's load coincidence (WLC) theory (Aktas *et al.* 2001; Wen 2001):

$$P_{fj} = 1 - e^{-[RR_j^D P_{fj}^D + RR_j^S P_{fj}^S + RR_j^{DS} P_{fj}^{DS}]} \quad (12)$$

where P_{fj} is the failure probability of pipeline j subjected to both seismic and deterioration loads; RR_j^{DS} is the estimated repair rate of pipeline j when deterioration and seismic hazards occur simultaneously; and P_{fj}^{DS} is the failure probability of pipeline j when deterioration and seismic hazards occur simultaneously. It should be noted that P_{fj} is the failure probability of pipeline j when subjected to both seismic and deterioration loads but not necessarily at the same time, while P_{fj}^{DS} is the failure probability of pipeline j for the occurrence of deterioration and seismic hazards simultaneously.

The combined repair rate (RR_j^{DS}) and fragility (P_{fj}^{DS}) of a given pipeline j is estimated using the following equations after assuming that seismic and deterioration hazards are independent events:

$$P_{fj}^{DS} = 1 - e^{-(RR_j^{DS})} \quad (13)$$

$$RR_j^{DS} = RR_j^S + RR_j^D \quad (14)$$

Furthermore, growth in water consumption demands is accounted for using the following equation:

$$q_{i,t,y}^* = q_{i,t,0}^* \left(1 + \frac{DRG}{100}\right)^y \quad (15)$$

where $q_{i,t,y}^*$ is the demand at node i at the end of a target year y ; $q_{i,t,0}^*$ is the current demand at node i ; DRG is the annual demand growth rate (percentage) which is assumed as 4% in this study.

DEMONSTRATION

Data for the WSS in the Charleston peninsula region in South Carolina are used to demonstrate the proposed pipeline rehabilitation framework (Farahmandfar *et al.* 2015). The layout of the WSS in the study area (hereafter CWSS) is depicted in Figure 1. CWSS comprises pipelines that add up to about 150 km (1 km = 0.62 mile) in length. CWSS has 1,474 demand nodes and 1,874 individual pipe segments. The majority of CWSS pipelines are made of either DI, CI, polyvinylchloride (PVC), or galvanized steel (GALV) materials and their sizes varied from 25.4 mm to 609.6 mm in diameter. Measured by length, DI accounted for about 72% of CWSS pipelines followed by CI with 20% and the rest accounted by PVC and GALV. Measured by length, 152.4 mm diameter pipelines accounted for most of about 47% of CWSS pipelines. A comprehensive review of CWSS features can be found in Piratla *et al.* (2014).

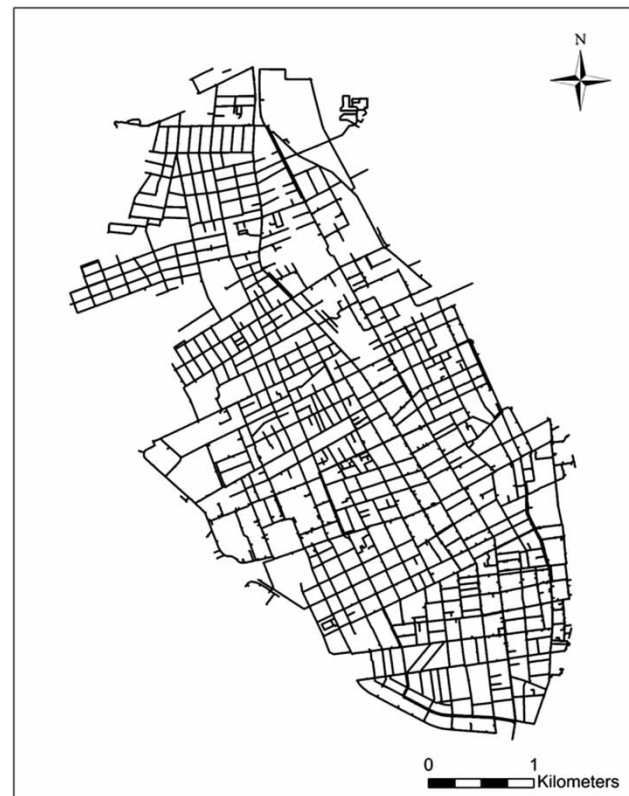


Figure 1 | Layout of the WSS in the Charleston peninsula region.

Estimated deterioration-related repair rates of CWSS pipelines are calculated using Equations (3) and (4) while the fragilities are estimated using Equation (10) (Farahmandfar 2016). A reasonable age of 50 years is assumed for CWSS pipelines due to lack of age data. Figure 2 presents the distribution of CWSS pipelines measured by length based on their deterioration fragilities. As per Figure 2, 71% of CWSS pipelines have fragility values of less than 20%. Furthermore, it is observed from the fragility estimates that the average fragility of DI pipeline segments of CWSS is about 7% more than that of CI pipelines.

Besides the deterioration vulnerability, it was evident from the 1886 earthquake that the CWSS region is also vulnerable to moderate to severe seismic activity (Robinson & Talwani 1983; Dutton 1889; Hayati & Andrus 2008). As a result, capital improvement planning for CWSS serves as an interesting case study where not only aging infrastructure issues need be addressed, but also measures ought to be taken to make CWSS more resilient to seismic hazards. The seismic repair rates (RR^S) along with seismic fragilities (Pf^S) are estimated for CWSS pipelines using Equations (7) and (11), respectively, following the procedure presented in Farahmandfar *et al.* (2016) after assuming a peak ground acceleration (PGA) of 0.3 g which corresponds to a M_W of ~7.

It should be noted that the map of liquefaction potential index (LPI) developed for the study region by Hayati & Andrus (2008) was used to derive the estimated seismic repair rates for CWSS pipelines. Liquefaction potential of a region is characterized using the estimated probability

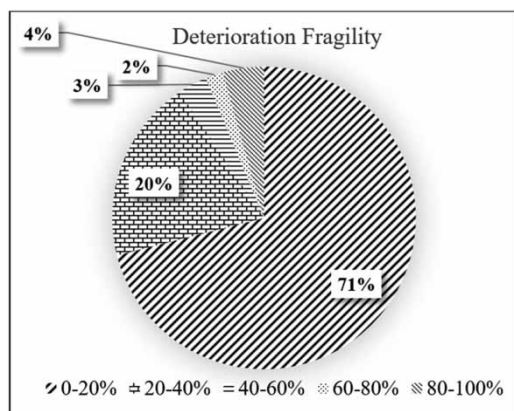


Figure 2 | Distribution of CWSS pipelines measured by length based on their deterioration fragilities.

that the LPI will be greater than 5 ($P_{LPI>5}$), which is the approximate threshold for sand boil generation (Toprak & Holzer 2003). The CWSS LPI map categorized the study region into the following three zones: (a) $P_{LPI>5} = 10\%$; (b) $P_{LPI>5} = 45\%$; and (c) $P_{LPI>5} = 95\%$. Such a categorization can be interpreted to mean that $P_{LPI>5} = 95\%$ zone is roughly two times as likely to liquefy as $P_{LPI>5} = 45\%$ zone (Farahmandfar *et al.* 2016). The seismic fragility distribution of CWSS pipelines by length is presented in Figure 3.

It can be seen from Figure 3 that about 43% of CWSS pipelines measured by length have seismic fragilities of less than 20% while only 4% have seismic fragilities of more than 80%. It is also observed that CI pipelines are more vulnerable to the seismic hazards with an average seismic fragility of 33% compared to DI pipelines with an average seismic fragility of 22%. The seismic fragilities did not seem considerably distinct for small and large diameter CWSS pipelines. It is also observed that the average seismic fragility of CWSS pipelines located in the 95% LPI zone is almost three times greater than that of the pipelines located in the 45% LPI zone. Expectedly, seismic fragility estimates are found to be highly sensitive to LPI values based on which they were derived (Farahmandfar *et al.* 2016).

The integrated pipeline fragilities due to the combined loading of deterioration and seismic hazards are calculated using Equations (12)–(14). Figure 4 illustrates the integrated fragilities of CWSS pipelines, while Figure 5 presents the distribution of CWSS pipelines measured by length based on their integrated fragilities. It is observed that the average

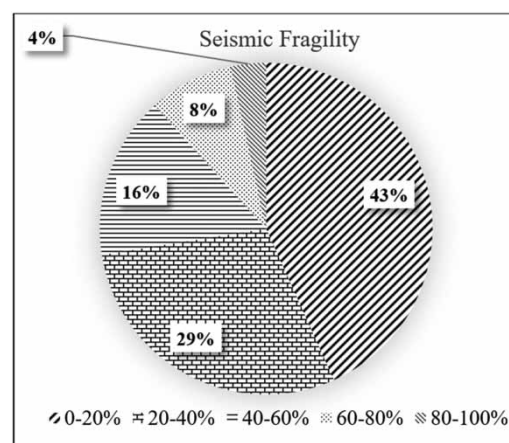


Figure 3 | Distribution of CWSS pipelines measured by length based on their seismic fragilities.

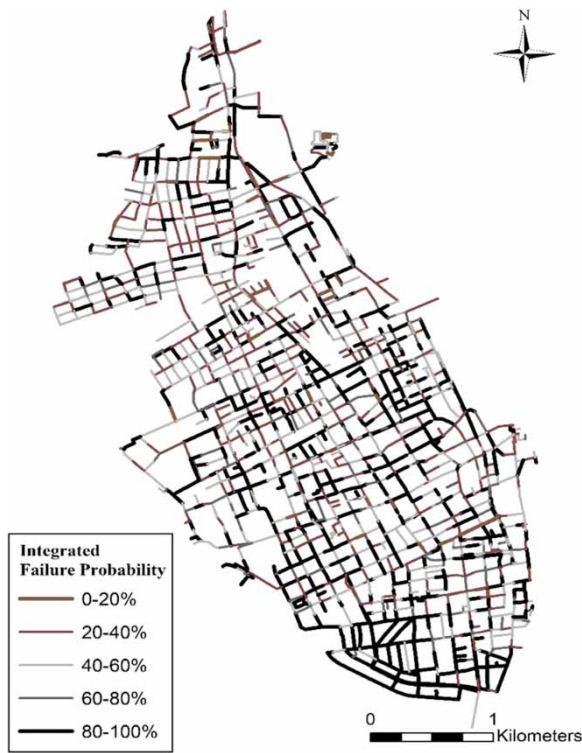


Figure 4 | Integrated fragilities of CWSS pipelines.

pipeline fragility due to the combined loading is 69%. Furthermore, it can be observed from Figure 5 that 44% of CWSS pipelines have very high (i.e., 80–100%) integrated fragilities, followed by 28% CWSS pipelines with moderate integrated fragilities (i.e., 40–60%). It is also observed that the average integrated fragility of CI pipelines is about

75% while it is 66% for DI pipelines. Similar to seismic fragility distribution, the average integrated fragility of smaller and larger diameter CWSS pipelines is found to be indistinct.

An optimization algorithm is used to determine the best rehabilitation strategies that will maximize the flow-based resilience of CWSS within given budgetary constraints when deterioration and seismic hazards are considered together. Three specific algorithms are tested in this study to determine their respective capabilities in producing the best solutions for various budget constraints. The first algorithm is GA comprising 150 generations per run, using a simple point crossover probability of 0.75, and a uniform mutation probability of 0.01. The second algorithm is SFLA with 50 iterations, 10 frogs per memeplex, and the memeplex size of 100 and the third algorithm is ABC with 50 iterations per run and colony size of 80 (Farahmandfar 2016).

Rehabilitation budgets ranging from \$25 million to \$30 million in increments of \$1 million are used as constraints in the optimization algorithms in various scenarios. The cost of rehabilitation is calculated using Equation (2), assuming relining cost of \$0.387/mm/m (\$0.387 per mm of diameter per meter of pipeline) (or \$3/inch/ft) and a replacement cost of \$1.04/mm/m (\$8/inch/ft) (Farahmandfar 2016). These unit costs are inflation-adjusted prices obtained from the literature, assuming that pipe bursting is used for replacement and cement mortar lining for relining (Boyce & Bried 1998). Lining a pipeline using the non-structural cement mortar lining method will result in significant improvement of the roughness (i.e., Hazen-Williams (C) coefficient (Deb *et al.* 1990). It is assumed that the C value of a pipeline after it has been lined would be 120. It is also assumed that the pipeline would be downsized by 15% with the lining option; although it should be noted that the liner thickness, in reality, would vary with the host pipe size depending on numerous other desired features. On the other hand, when a pipeline is replaced, not only will its Hazen-Williams coefficient increase (Kleiner *et al.* 1998) but also its structural capacity will be enhanced (or fragility improved). It is assumed that the C value of a replaced pipeline would be 140 which is a typical value for new flexible pipelines. It is also assumed that the pipelines selected will be replaced with flexible pipe materials

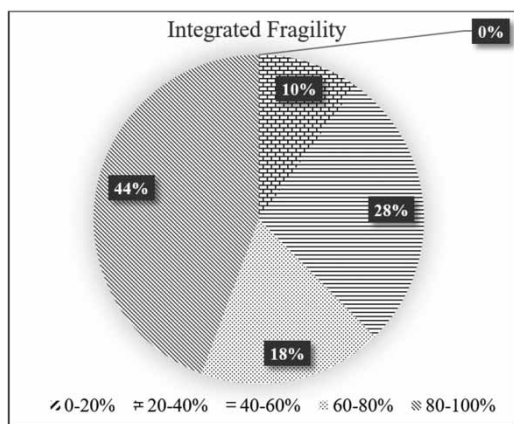


Figure 5 | Distribution of CWSS pipelines measured by length based on their integrated fragilities.

Table 1 | Summary of the rehabilitation features

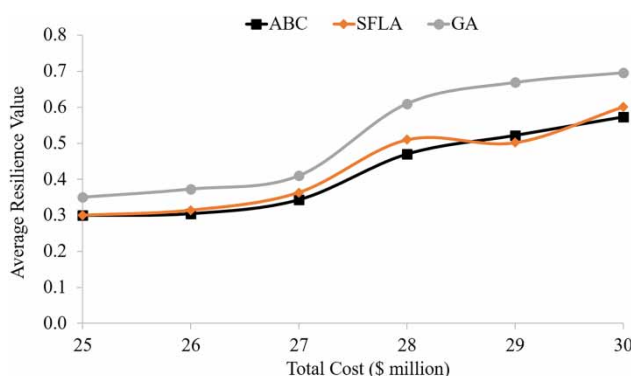
Rehabilitation action	Diameter	Hazen–Williams coefficient	Failure probability
Relining	Decreases by 15%	Increases to 120	Does not change
Replacement with same diameter pipeline	Does not change	Increases to 140	Decreases to the failure probability of the replaced pipeline
Replacement with larger diameter pipeline	Increases by 101.6 mm	Increases to 140	Decreases to the failure probability of the replaced pipeline

(e.g., DI) (Farahmandfar 2016). **Table 1** summarizes the rehabilitation features used in this study.

The optimization algorithms are integrated with EPANET 2.0 using its toolkit library in the MATLAB programming environment in order to quantify the flow-based resilience of CWSS using Equation (1). **Figure 6** presents the resilience improvement trends of the three algorithms for various budget constraints based on the best solutions obtained over five separate runs of each algorithm. It can be observed from **Figure 6** that GA performed better than SFLA and ABC algorithms and, consequently, it is chosen to be used in the proposed rehabilitation framework.

The GA-based rehabilitation framework is used to further investigate the types of pipelines selected for rehabilitation in cases of (a) only deterioration, (b) only seismic, and (c) a combination of deterioration and seismic hazards. The results corresponding to a budget constraint of \$30 million are used in this paper for discussing the comparative analysis of various hazard scenarios and the resulting sets of rehabilitation choices.

Figure 7 presents the distributions of CWSS pipelines measured by length that are selected for each rehabilitation

**Figure 6** | Comparison of maximum resilience values produced by the three optimization algorithms for various budget constraints.

alternative for each hazard scenario. Similarly, budget distributions for different rehabilitation alternatives are presented in **Figure 8**.

It can be observed from **Figures 7** and **8** that all the three hazard scenarios have somewhat comparable distributions of pipeline length and budget spent on the three rehabilitation alternatives. It is, however, observed that the actual pipelines selected for rehabilitation are considerably different for each hazard scenario; although somewhat similar in characterization. The observed difference is quantified using a *percentage difference* parameter. Percentage difference represents how different rehabilitation strategies are for a given pair of hazard scenarios and it is calculated as the ratio of summation of the length of pipelines with different rehabilitation plans for any two hazard scenarios to the summation of the length of all CWSS pipelines using the following equation:

$$PD^{m,n} = \frac{\sum_{i=1}^{N_p} (L_j^{m,n})}{\sum_{j=1}^{N_p} (L_j)} \times 100\% \quad (16)$$

where $PD^{m,n}$ is the percentage difference between hazard scenarios m and n ; N_p is the total number of CWSS pipelines; L_j is the length of pipe j ; and $L_j^{m,n}$ is 0 if rehabilitation strategies of pipe j in m and n hazard scenarios are the same, while it is equal to L_j if rehabilitation strategies of pipe j in m and n hazard scenarios are different.

It can be seen from **Table 2** that the percentage differences in rehabilitation strategies for multiple pairs of hazard scenarios are considerably significant. Although the percentage differences are significant, several similarities existed in the characteristics of the pipelines chosen for rehabilitation in multiple hazards. The three hazard scenarios are theoretically different in the way the pipeline fragilities (i.e., $\sum_{j=1}^{N_p} (1 - P_{fj})$ in Equation (1)) are estimated.

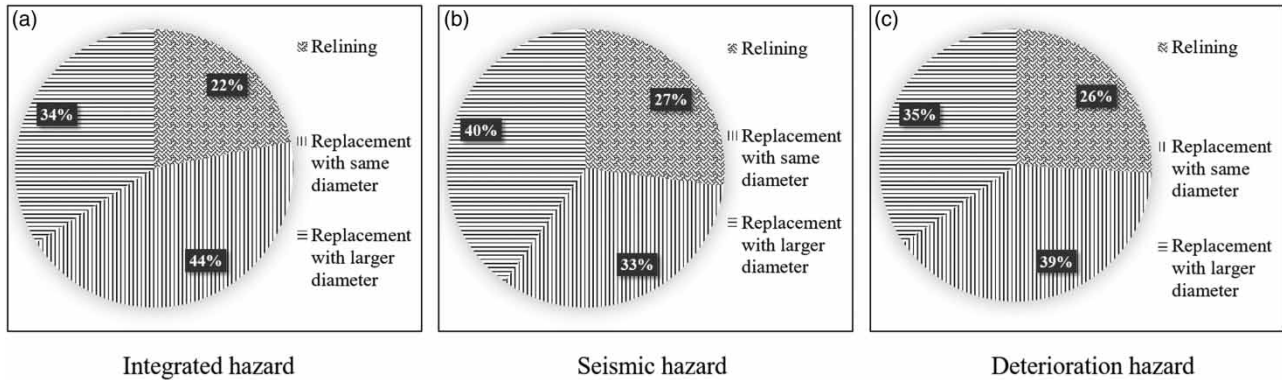


Figure 7 | Distribution of pipelines by length in each rehabilitation category.

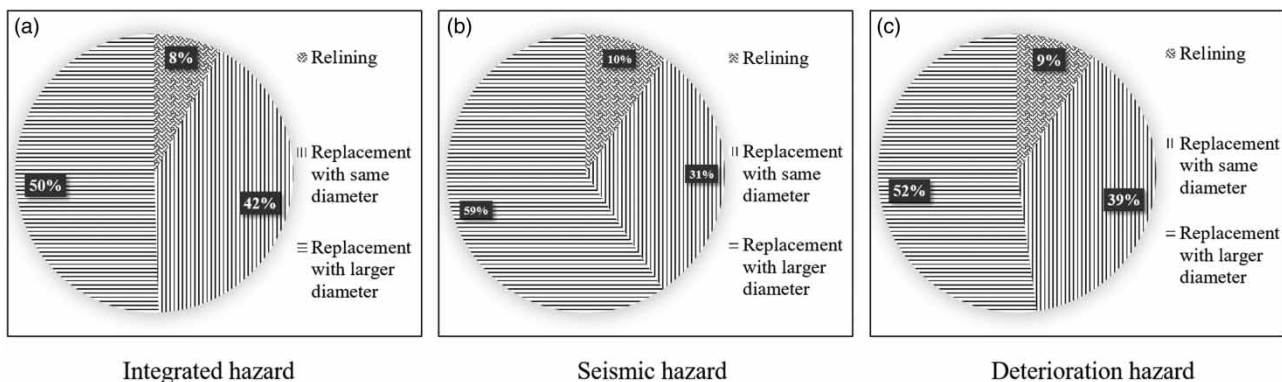


Figure 8 | Budget spent on different rehabilitation actions.

Table 2 | Percentage differences in rehabilitation preferences between pairs of hazard scenarios

Hazard scenarios	% Differences
Integrated and deterioration hazards	41%
Deterioration and seismic hazards	70%
Integrated and seismic hazards	70%

The buffer head component $(h_{i,t} - h_{i,t}^*)$ in Equation (1) is not expected to contribute significantly towards variation in rehabilitation solutions because it is independent of the hazard scenario. Therefore, variation in the rehabilitation solutions for different hazard scenarios is expected to be dependent on how much influence the fragility parameter has on the resilience metric. The observed variation in the rehabilitation solutions is correlated with the variation in the fragility estimates for each hazard scenario to better identify the characteristics of pipelines whose rehabilitation

will maximize the system resilience for each hazard scenario.

As per Table 1, the 'relining' alternative does not change the fragility of a pipeline and therefore would not result in considerable variation across the three hazard scenarios. Consequently, only those pipelines selected for 'replacement' are analyzed. It should be noted that the obtained rehabilitation solutions may be influenced by the fact that the majority of CWSS pipelines are of similar length, diameter, material, and are located in the same LPI zone. Comparing entire sets of rehabilitated pipelines may, therefore, result in misleading interpretations with inherent bias towards populous pipeline features. Consequently, in an attempt to carry out an unbiased analysis, pipelines are categorized into various homogenous groups for correlating their replacement selection with estimated fragility improvements for the three hazard scenarios in a normalized manner. A homogenous group of pipelines are made of the same material, are of

Table 3 | Characteristics of homogenous pipeline groups

Group number	Length of CWSS pipelines in the group (km)	Material	Length	LPI zone
1	33.5	DI	≤ 100 m	45%
2	42.6	DI	≥ 100 m	45%
3	16.6	DI	≤ 100 m	95%
4	16.0	DI	≥ 100 m	95%
5	12.5	CI	≤ 100 m	45%
6	13.4	CI	≥ 100 m	45%
7	3.8	CI	≤ 100 m	95%
8	4.7	CI	≥ 100 m	95%

similar length, and located in the same LPI zone. As shown in **Table 3**, CWSS pipelines are categorized into eight homogenous groups. Pipelines adding up to about 1.6 km (or 1 mile) of length are randomly selected from each homogenous group for the comparative analysis in order to nullify the effect of populous groups. The random selection process is repeated 1,000 times to avoid unintended selection biases. Subsequently, the average *replacement rate* is calculated for each homogeneous group over the 1,000 simulations. *Replacement rate* is the ratio of summation of the length of replaced pipelines to the summation of length (i.e., 1.6 km) of all the selected pipelines in each simulation for a given homogenous group. Results from replacement ratio are separately discussed for each hazard scenario.

Only-deterioration hazard

Assuming 50 years as the age of CWSS pipelines, it is observed from analyzing the deterioration fragility Equations (3), (4), and (6) that fragility improvement upon replacement is greater for CI pipelines than DI pipelines of short lengths and small diameters. It is also observed from analyzing the fragility equations that fragility improvement would increase significantly with length in the case of DI pipelines while it would decrease marginally in the case of CI pipelines. Consequently, with increasing pipeline length, DI pipelines would fare better than CI pipelines in terms of fragility improvement. Furthermore, it is observed that fragility improvement decreased with increasing diameter for both CI and DI pipelines. On the other hand, it is clearly evident from the fragility equations that deterioration

fragility improvement does not depend on the LPI probability of replaced pipeline's location. Replacement strategies determined for the deterioration hazard are summarized in **Figure 9** using the distributions of replaced CWSS pipeline diameters, materials, and LPI values measured by length.

As per **Figure 9**, many CWSS pipelines selected for replacement are DI pipelines, with less than 152.4 mm diameter, and located in the 45% liquefaction (LPI) zone. This result may be biased due to the fact that smaller diameter DI pipelines, located in the 45% liquefaction (LPI) zone account for the highest share of water mains by length in CWSS. Consequently, average *replacement rates* of all the homogenous pipeline groups identified in **Table 3** are analyzed in comparison with expected and observed fragility improvements. The results of such analysis are presented in **Table 4**.

Consistent with the expectation, homogenous groups 2 and 4 corresponding to DI pipelines of longer lengths produced greatest fragility improvement and also greatest replacement rates among the eight groups. This observation validates the hypotheses that DI pipelines of longer lengths would result in greater fragility improvement than both DI pipelines of shorter lengths and CI pipelines of similar lengths. Also as expected, fragility improvement of CI pipelines (from homogenous groups 5, 6, 7, and 8) reduced marginally, if at all there was any reduction, with increased length, and the variation in replacement rate seemed inconsistent with respect to the variation in length. It should be noted that the proportion of pipelines selected for replacement from each homogenous group also depends on their respective locations in CWSS and their resulting influence on the buffer head component of the resilience calculation. Furthermore, there are not any significant differences in fragility improvements and replacement rates between homogenous groups corresponding to different LPI zones.

Only-seismic hazard

Based on seismic fragility Equations (7)–(9), it can be seen that K_1 and K_2 take their highest values for CI pipelines and least for DI pipelines. Therefore, replacing CI pipelines will decrease K_1 and K_2 by 50% while replacing DI pipelines will not change these factors. In other words, replacing CI

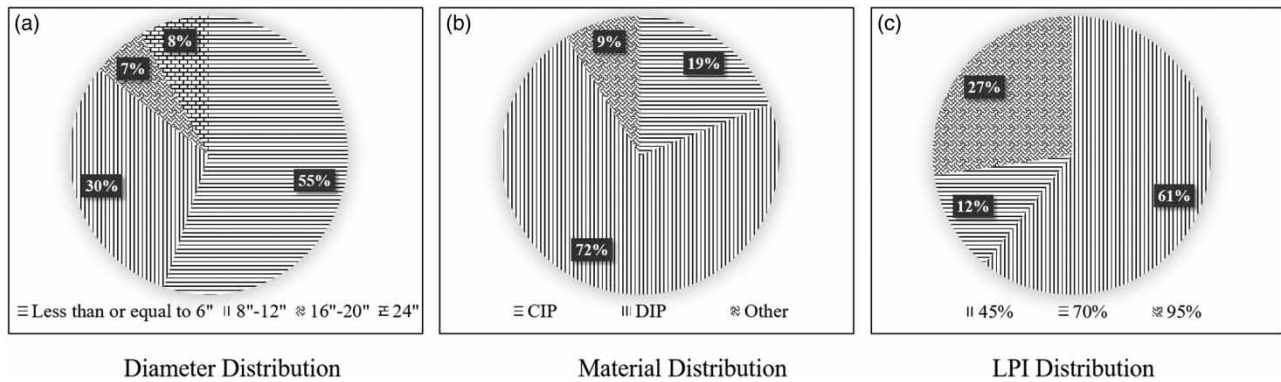


Figure 9 | Distribution of pipelines by length selected for both 'replacement' alternatives in the case of deterioration hazard scenario.

Table 4 | CWSS pipeline rehabilitation preferences for deterioration hazard

Group number	Replacement rate	Average fragility improvement
1	50%	8%
2	57%	28%
3	55%	8%
4	62%	25%
5	51%	9%
6	42%	9%
7	36%	10%
8	41%	8%

pipelines produces higher fragility improvement than DI pipelines. The fragility improvement is also observed to be increasing with pipeline length. Also, replacing pipelines with at least one previous break produced higher fragility improvement than replacing pipelines with no previous breaks. Furthermore, it is observed from analyzing the seismic fragility equations that replacing CI pipelines in the 95%

LPI zone produced greater fragility improvement than replacing CI pipelines in the 45% LPI zone. The distribution of CWSS pipelines' diameter, material, and LPI probabilities measured by length that are selected for both replacement alternatives (i.e., replace with same diameter and replace with larger diameter) in the case of seismic hazard scenario are presented in [Figure 10](#).

It can be seen from [Figure 10](#) that the majority of selected pipelines for replacement are the populous smaller diameter DI pipelines that are located in the 45% LPI zone. The results of the homogenous groups are further analyzed, as shown in [Table 5](#), to identify suitable pipeline characteristics that will aid resilience enhancement for seismic hazards.

It can be clearly observed from [Table 5](#) that fragility improvement percentages as well as pipeline replacement rates are higher for CI pipelines (groups 5–8) than DI (groups 1–4), as expected, due to their rigid nature. It can also be noted from the results in [Table 5](#) that pipeline

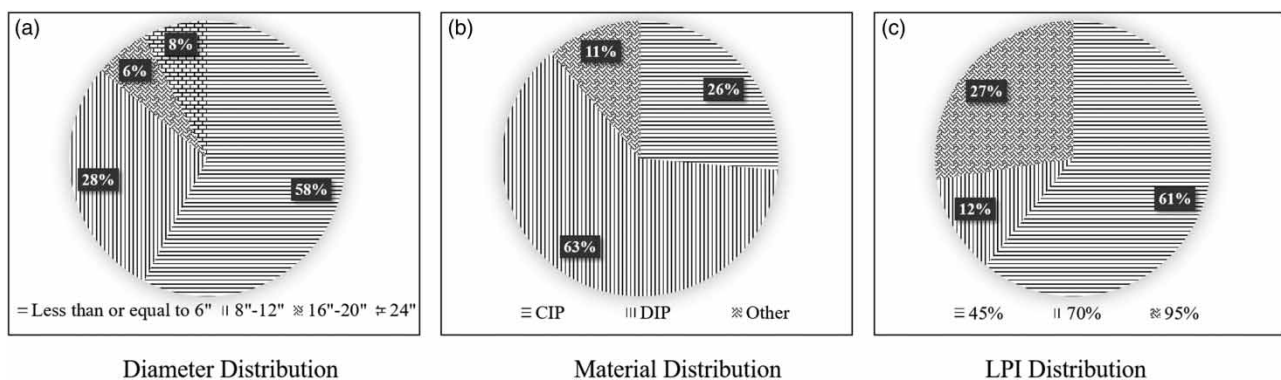


Figure 10 | Distribution of pipelines by length selected for both 'replacement' alternatives in the case of seismic hazard scenario.

Table 5 | CWSS pipeline rehabilitation preferences for seismic hazard

Group number	Replacement rate	Average fragility improvement
1	48%	1%
2	47%	3%
3	54%	4%
4	44%	3%
5	64%	9%
6	62%	16%
7	54%	26%
8	66%	29%

fragility improvement increased with pipeline length for CI pipelines, as expected; however, the pipeline replacement rates are a little inconsistent for the 45% LPI zone which could be due to the criticality of shorter length CI pipelines located in this zone in terms of their greater influence on the hydraulic buffer head of the resilience calculations. Furthermore, as expected, fragility improvement of homogenous groups corresponding to CI pipelines located in the 95% LPI zone (groups 7 and 8) is greater than that of CI pipelines located in the 45% LPI zone (groups 4 and 5).

Integrated hazard scenario

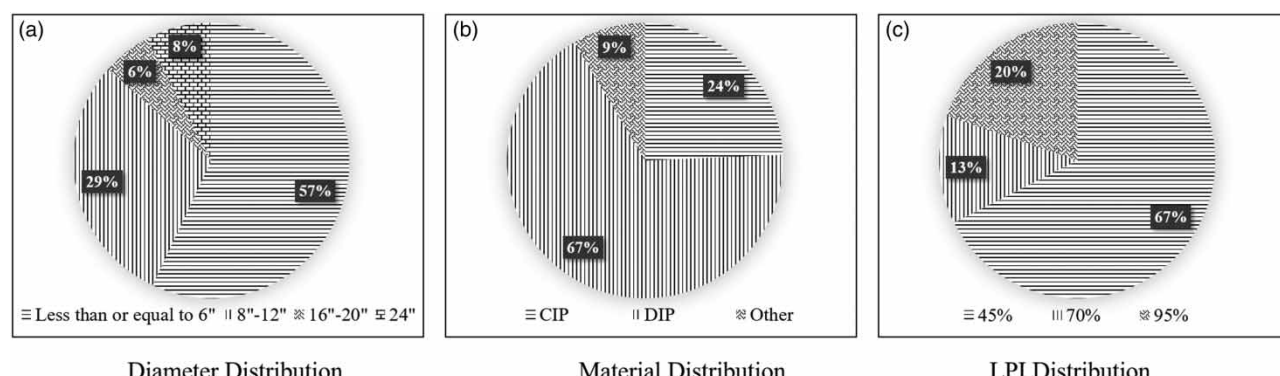
Integrated pipeline fragilities calculated using Equations (12)–(14) are dependent on both seismic and deterioration pipeline fragilities. It is observed from analyzing the integrated fragility equations that fragility improvement is higher for shorter CI pipelines than shorter DI pipelines whereas for longer (much longer than 100 m) segments, replacing DI pipelines resulted in higher fragility

improvement. It is also observed that fragility improvement is greater for DI pipelines located in the 45% LPI zone than those located in the 95% LPI zone. Furthermore, fragility improvement in replacing CI pipelines with at least one previous break is higher than DI pipelines with a similar number of previous breaks. The distribution of replaced CWSS pipelines' diameters, materials, and LPI values measured by length in the integrated hazard scenario is shown in Figure 11. The replacement rates of various homogenous pipeline groups for the integrated hazard are shown in Table 6.

It can be seen from Table 6 that homogenous groups representing pipelines located in the 45% LPI zone produced the greatest fragility improvement which translated into higher replacement rates. It can also be seen from Table 6 (groups 1, 3, 5, and 7) that fragility improvement is higher for shorter CI pipelines than shorter DI pipelines and also that the replacement rates are consistent with the trend of fragility improvement for all the homogenous groups.

Table 6 | CWSS pipeline rehabilitation preferences for integrated hazard

Group number	Replacement rate	Average fragility improvement
1	59%	30%
2	58%	45%
3	47%	8%
4	37%	7%
5	74%	51%
6	61%	43%
7	49%	15%
8	40%	11%

**Figure 11** | Distribution of pipelines by length selected for both 'replacement' alternatives in the case of integrated hazard scenario.

CONCLUSIONS AND RECOMMENDATIONS

This paper presented and demonstrated a water main rehabilitation framework that simultaneously accounts for estimated growth in water demand as well as vulnerabilities due to seismic hazards and pipeline deterioration. The WSS serving an earthquake-prone region in South Carolina is used in this study for demonstration purposes. The proposed rehabilitation planning framework is driven by a GA that maximizes WSS resilience. Pipeline rehabilitation actions including relining, replacement with the same diameter pipeline, replacement with larger diameter pipeline, and leaving as it is are considered as part of the proposed framework. The optimal rehabilitation actions resulted for various hazard scenarios are compared to illustrate their differences. Although the majority of pipelines selected for rehabilitation against different hazards shared similar characteristics, the actual pipelines selected were considerably different as evidenced by the high percentage differences. It was observed that replacing longer segments of DI pipelines resulted in greater resilience enhancement of the studied WSS for deterioration hazard and that such resilience benefits increased with the length of replaced DI pipe segments. Furthermore, it was observed that replacing CI pipelines, especially those located in the 95% LPI zone, produced the greatest resilience benefits for the seismic hazard. It was also observed that the fragility improvement is highly correlated with replacement rates across the homogenous groups for the integrated hazard. It was noted that short CI pipe segments located in the 45% LPI zone and long CI segments located in the 95% LPI zone may be critically located in the studied WSS to influence their selection for replacement through higher contribution to buffer head improvement.

The research limitations that may be addressed in the future include: (a) the lack of consideration for the type of pipeline joints which could also influence the behavior of WSSs during earthquakes; (b) the lack of real age data for the pipelines and the subsequent assumption of the same age for all CWSS pipelines; and (c) the assumptions made in resilience improvement capabilities of each rehabilitation action. Furthermore, it should be noted that the unit costs of pipe lining and replacement used in this study are estimated based on an old reference. Although the older estimates are appropriately adjusted for inflation, they are very likely

lower than the current prevailing prices and, therefore, those unit cost estimates need to be cautiously interpreted.

ACKNOWLEDGEMENTS

The support of the National Science Foundation (NSF) under Grant No. 1638321 is greatly appreciated. The views and conclusions contained in this document are those of the authors and should not be interpreted as necessarily representing the official policies, either expressed or implied, of the United States Government.

REFERENCES

Aktas, E., Moses, F. & Ghosn, M. 2009 *Cost and safety optimization of structural design specifications*. *Reliability Engineering & System Safety* **73** (3), 205–212.

ALA 2009 American Lifelines Alliance: seismic fragility formulations for water systems-guideline and appendices. http://www.americanlifelinesalliance.com/pdf/Part_1_Guideline.pdf (accessed 29 March 2017).

Alvisi, S. & Franchini, M. 2006 *Near-optimal rehabilitation scheduling of water distribution systems based on a multi-objective genetic algorithm*. *Civil Engineering and Environmental Systems* **23** (3), 143–160.

Andreou, S. A., Marks, D. H. & Clark, R. M. 1987 *A new methodology for modelling break failure patterns in deteriorating water distribution systems: theory*. *Advances in Water Resources* **10** (1), 2–10.

Ariaratnam, S. T. & Sihabuddin, S. 2009 *Comparison of emitted emissions between trenchless pipe replacement and open cut utility construction*. *Journal of Green Building* **4** (2), 126–140.

Ariaratnam, S. T., Piratla, K., Cohen, A. & Olson, M. 2013 *Quantification of sustainability index for underground utility infrastructure projects*. *Journal of Construction Engineering and Management* **139** (12), A4013002.

ASCE 2017 Infrastructure Report Card. <http://www.infrastructurereportcard.org/wp-content/uploads/2017/01/Drinking-Water-Final.pdf> (accessed 29 March, 2017).

Boyce, G. M. & Bried, E. M. 1998 Social cost accounting for trenchless projects. In: *North American No-Dig Conference '98*. Albuquerque, NM, pp. 2–12.

Bruneau, M., Chang, S. E., Eguchi, R. T., Lee, G. C., O'Rourke, T. D., Reinhorn, A. M. & Von Winterfeldt, D. 2003 *A framework to quantitatively assess and enhance the seismic resilience of communities*. *Earthquake Spectra* **19** (4), 733–752.

Cimellaro, G. P., Tinebra, A., Renschler, C. & Fragiadakis, M. 2015 *New resilience index for urban water distribution networks*. *Journal of Structural Engineering* **142** (8), C4015014.

Dandy, G. C. & Engelhardt, M. 2001 *Optimal scheduling of water pipe replacement using genetic algorithms*. *Journal of Water Resources Planning and Management* **127** (4), 214–223.

Dandy, G. C. & Engelhardt, M. 2006 *Multi-objective trade-offs between cost and reliability in the replacement of water mains*. *Journal of Water Resources Planning and Management* **132** (2), 79–88.

Deb, A. K., Snyder, J. K., Chelius, J. J. & O'Day, D. K. 1990 *Assessment of Existing and Developing Water Main Rehabilitation Practices*. American Water Works Association Research Foundation, Denver, CO.

Deb, A. K., McCammon, S. B., Snyder, J. & Dietrich, A. M. 2010 *Impacts of Lining Material on Water Quality [Project# 4036]*. Water Research Foundation, Denver, CO.

Dutton, C. E. 1889 *The Charleston Earthquake of August 31, 1886. USGS Ninth Annual Report, 1887–1888*. US Geological Survey, Washington, DC, pp. 203–528.

Farahmandfar, Z. 2016 *Resilience-based Rehabilitation Planning for Water Distribution Systems in Seismic Zones*. PhD Dissertation, Clemson University, Clemson, SC.

Farahmandfar, Z., Piratla, K. R. & Andrus, R. D. 2015 Flow-based modeling for enhancing seismic resilience of water supply systems. In: *Pipelines Conference 2015. American Society of Civil Engineers (ASCE)*, Baltimore, MD, pp. 756–765.

Farahmandfar, Z., Piratla, K. R. & Andrus, R. D. 2016 *Resilience evaluation of water supply systems against seismic hazards*. *ASCE Journal of Pipeline Systems Engineering and Practice* **8** (1), 04016014.

Fragiadakis, M. & Christodoulou, S. E. 2014 *Seismic reliability assessment of urban water networks*. *Earthquake Engineering & Structural Dynamics* **43** (3), 357–374.

Halhal, D., Walters, G. A., Ouazar, D. & Savic, D. A. 1997 *Water network rehabilitation with structured messy genetic algorithm*. *Journal of Water Resources Planning and Management* **123** (3), 137–146.

Hayati, H. & Andrus, R. D. 2008 *Liquefaction potential map of Charleston, South Carolina based on the 1886 earthquake*. *Journal of Geotechnical and Geoenvironmental Engineering* **134** (6), 815–828.

Karaboga, D. & Akay, B. 2009 *A comparative study of artificial bee colony algorithm*. *Applied Mathematics and Computation* **214** (1), 108–132.

Kleiner, Y. & Rajani, B. 2001 *Comprehensive review of structural deterioration of water mains: statistical models*. *Urban Water* **3** (3), 131–150.

Kleiner, Y., Adams, B. J. & Rogers, J. S. 1998 *Long-term planning methodology for water distribution system rehabilitation*. *Water Resources Research* **34** (8), 2039–2051.

Nafi, A. & Kleiner, Y. 2010 *Scheduling renewal of water pipes while considering adjacency of infrastructure works and economies of scale*. *Journal of Water Resources Planning and Management* **136** (5), 519–530.

Piratla, K. R., Fisher, K. E., Andrus, R. D., Simonson, L. A. & Farahmandfar, Z. 2014 Evaluating the resiliency of the water system in Charleston, South Carolina against liquefaction hazard through the use of seismic hazard maps. In: *Proceedings of the ASCE Pipelines 2014 Conference*, Portland, OR.

Piratla, K. R., Matthews, J. C. & Farahmandfar, Z. 2016 The role of resilience in the rehabilitation planning of water pipeline systems. In: *Proceedings of the ASCE Pipelines 2016 Conference*, Kansas City, MO, pp. 1856–1864.

Prasad, T. D. & Park, N. S. 2004 *Multi objective genetic algorithms for design of water distribution networks*. *Journal of Water Resources Planning and Management* **130** (1), 73–82.

Robinson, A. & Talwani, P. 1983 Building damage at Charleston, South Carolina, associated with the 1886 earthquake. *Bulletin of the Seismological Society of America* **73** (2), 633–652.

Rossmann, L. A. 2000 *EPANET2: User's Manual*. US Environmental Protection Agency, National Risk Management Research Laboratory, Cincinnati, OH.

Selvakumar, A., Clark, R. M. & Sivaganesan, M. 2002 *Costs for water supply distribution system rehabilitation*. *Journal of Water Resources Planning and Management* **128** (4), 303–306.

Shamir, U. & Howard, C. D. D. 1979 An analytic approach to scheduling pipe replacement. *Journal of the American Water Works Association* **71** (5), 248–258.

Su, Y. C., Mays, L. W., Duan, N. & Lansey, K. E. 1987 *Reliability based optimization model for water distribution systems*. *Journal of Hydraulic Engineering* **113** (12), 1539–1556.

Tanyimboh, T. T. & Templeman, A. B. 2000 *A quantified assessment of the relationship between the reliability and entropy of water distribution systems*. *Engineering Optimization* **33** (2), 179–199.

Todini, E. 2000 *Looped water distribution networks design using a resilience index based heuristic approach*. *Urban Water* **2** (2), 115–122.

Toprak, S. & Holzer, T. L. 2003 *Liquefaction potential index: field assessment*. *Journal of Geotechnical and Geoenvironmental Engineering* **129** (4), 315–322.

Walski, M. & Pelliccia, A. 1982 *Economic analysis of water main breaks*. *Journal of the American Water Works Association* **74** (3), 140–147.

Wang, Y., Zayed, T. & Mosehli, O. 2009 *Prediction models for annual break rates of water mains*. *Journal of Performance of Constructed Facilities* **23** (1), 47–54.

Wen, Y. K. 2001 *Minimum lifecycle cost design under multiple hazards*. *Reliability Engineering & System Safety* **73** (3), 223–231.

Woodburn, J., Lansey, K. E. & Mays, L. W. 1987 Model for the optimal rehabilitation and replacement of water distribution system components. In: *ASCE*, pp. 606–611.

Yoo, D. G., Kang, D., Jun, H. & Kim, J. H. 2014 *Rehabilitation priority determination of water pipes based on hydraulic importance*. *Water* **6** (12), 3864–3887.